

THERMODYNAMICS OF SYMPORT AND ANTIPOINT CATALYZED BY CLONED OR NATIVE TRANSPORTERS

GEORGE A. GERENCSEK AND BRUCE R. STEVENS

*Department of Physiology, College of Medicine, University of Florida, Gainesville,
FL 32610-0274, USA*

Summary

Thermodynamic measurements are required to confirm whether cloned transport-associated proteins in a membrane truly constitute a functional transport system. Symport or antiport, catalyzed by native systems or by cloned proteins in membranes, can lead to steady-state intracellular accumulation of solute when the electrochemical potentials of activator ion and solute are energetically coupled. Secondary active transport can occur if an appropriate physical coupling mechanism exists in the membrane. Driving forces for secondary active transport are ultimately established by primary active transport or respiration. Steep steady-state gradients of solute can be maintained when the ion:solute coupling ratio is greater than one and/or when coupling includes an electrical component. Although the steady-state accumulation of substrate is independent of the exact physical mechanism of transport, non-equilibrium and equilibrium transport kinetics aid in interpreting the rate, direction (symport *versus* antiport) and control of ion-coupled flux across a membrane. In some cases, the activator ion's chemical gradient alone is energetically adequate to maintain steady-state intracellular accumulation of solute, as demonstrated in invertebrate epithelial cells. To interpret accumulation ratios accurately, it is necessary to measure the intracellular activity coefficients for ions. For example, liquid ion-exchange microelectrode measurements demonstrate that over 30% of intracellular Na⁺ can be sequestered in epithelial cells.

Introduction

Physical and kinetic models of symport or antiport are often developed in conjunction with thermodynamic arguments that support the concept of secondary active transport. In this review, we discuss the energetics of ion-coupled solute active transport catalyzed by native transport systems or by membrane proteins encoded by cDNAs associated with transport. We show that secondary active transport models can be supported by experimentally measuring accumulation gradients of solute and activator ion, transmembrane electrical potentials and rates of flux or charge transfer. Finally, an invertebrate cell model is used to examine the energetic adequacy of the separate electrical and chemical components of a Na⁺ gradient in maintaining high cellular accumulation gradients of amino acids or sugars.

The current literature regarding cloned transporter proteins and native transport systems vindicates the pioneering transport concepts of Christensen, Crane, Kaback,

Key words: ion-coupled transport, active transport, thermodynamics, symport, antiport, secondary active transport, membrane transport, cloned transporters.

Mitchell and others. Christensen (1990) and colleagues (Christensen and Riggs, 1952; Riggs *et al.* 1958) initially proposed that ion gradients across plasma membranes could energize organic solute transport and accumulation in eukaryotic cells. They initially postulated that a physical mechanism might exist in the membrane to catalyze the energetic coupling of neutral amino acid influx to K^+ efflux. A few years later, Crane proposed a model that described Na^+ -activated glucose uptake in the small intestine (Crane *et al.* 1961). The Crane model was further developed for sugars and amino acids by Curran, Schultz and others (see reviews by Crane, 1977; Schultz, 1980; Kimmich, 1990; Kessler and Semenza, 1983; Schultz and Curran, 1970; Stevens, 1992*a,b*; Stevens *et al.* 1984; Wright, 1993; Kilberg *et al.* 1993). Kaback developed the model of prokaryotic β -galactoside/ H^+ symport (e.g. *Escherichia coli* lactose permease) as a similar paradigm associated with the chemiosmotic concept of Mitchell (Mitchell, 1961, 1991; Kaback *et al.* 1993). Several sources contribute to our current understanding of ion-activated transport: Crane's sodium-coupled sugar or amino acid symport was confirmed in epithelial membranes of intestine and renal proximal tubule (cloned proteins typified by the eukaryote SGLT1 family); the β -galactoside/ H^+ symport mechanism in *E. coli* has been examined using cloned proteins typified by the lactose permease of bacteria; and the emergence of a superfamily of neurotransmitter transport systems that are energized by Na^+ , K^+ and/or Cl^- (typified by the GAT isoforms and the GLAST-1 and EAAC1 expression clones). The extensive molecular characterization of β -galactoside/ H^+ symport perhaps gives this system the edge as the archetypal symporter. The following discussion concerning ion-coupled organic solute transport is applicable to virtually any secondary active transport system selective for such substrates as neurotransmitters, dipeptides, drugs, antibiotics, nucleotides, phosphate, sulfate, chloride and bicarbonate.

Identifying active transport

For passive diffusion, the rate of solute influx or efflux is proportional to the substrate's electrochemical potential difference ($\Delta\bar{\mu}$) across the membrane; at equilibrium the net flux (J) is zero and the electrochemical gradient collapses (i.e. $\Delta\bar{\mu}_S=0$ and $J=0$). Fig. 1 shows an example of simple passive diffusion of a solute transported across the membrane, following Fick's law, with the flux curve passing through the origin at $\Delta\bar{\mu}_S=0$. This example involves the simplest case of a non-charged solute S , so that electrical potentials do not play a role and $\Delta\bar{\mu}_S=\Delta\mu_S$. If energy can be coupled to the transport process, then 'active transport' could occur, and this would be operationally defined at equilibrium as a shift in the curve of Fig. 1 such that $J>0$ when $\Delta\bar{\mu}_S=0$ or, alternatively, $\Delta\bar{\mu}_S>0$ when $J=0$.

Secondary active transport

The direct coupling of energy to a solute flux, usually by dephosphorylation of ATP, is called primary active transport. This mode of transport is largely responsible for generating the asymmetric distribution of Na^+ , K^+ , H^+ and other ions across cell membranes. The electrochemical gradients generated by primary active transport can be coupled to the flux of other solute species; the subsequent uphill transport of a given

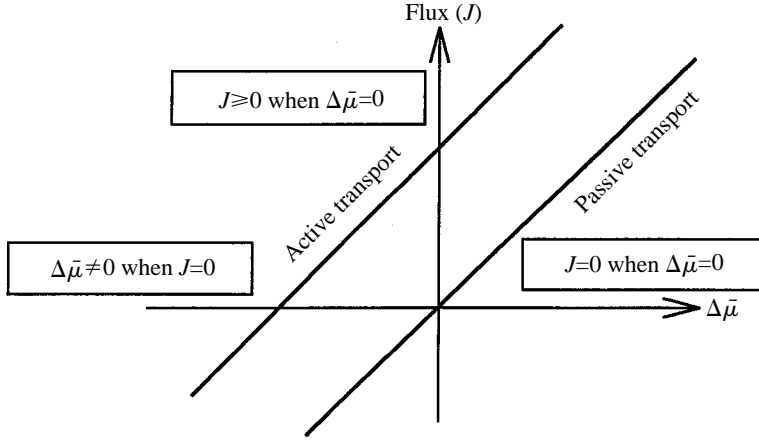


Fig. 1. Passive and active transport of solute S . The influx or efflux of S at equilibrium (J_s) is influenced by the electrochemical potential of S across the membrane ($\Delta\bar{\mu}_s$).

solute at the energetic expense of the other solute's electrochemical potential is called secondary active transport. Ion-coupled organic solute symport represents an example of secondary active transport. Alternatively, in bacterial or mitochondrial membranes, generation of $\Delta\bar{\mu}_H$, which arises by respiration, can be used to couple solute symport or antiport of other ions and organic solutes.

Energetic coupling

The coupling of energy can be described in terms of both equilibrium and non-equilibrium thermodynamics (Heinz *et al.* 1972; Kedem, 1978; Stein, 1986; Schultz, 1980; Onsager, 1931; Katchalsky, 1960). First, we provide a brief phenomenological description of energy coupling of an uncharged solute (S) with an activator cation that is independent of the actual transport mechanism. Following this, we present an example of a physical mechanism that can catalyze energy coupling in a membrane. The discussion is focused on simple ion-energized symport, but the arguments are applicable to virtually any system of symport or antiport, or to a combination of the two.

For symported species, continual fluxes in non-equilibrium conditions are related to forces by:

$$J_S = \Delta\mu_S \times L_{S,S} + \Delta\bar{\mu}_{ion} \times L_{S,ion}, \quad (1)$$

$$J_{ion} = \Delta\mu_S \times L_{ion,S} + \Delta\bar{\mu}_{ion} \times L_{ion,ion}, \quad (2)$$

where the conjugate driving forces behind the respective fluxes J_S and J_{ion} are represented by $\Delta\mu_S = RT \ln([S]^i/[S]^o)$ and $\Delta\bar{\mu}_{ion} = RT \ln([ion]^o/[ion]^i) - zF\Delta\Psi$, where F is the Faraday constant, $\Delta\Psi$ is the membrane electrical potential difference, R is the gas constant, T is absolute temperature and z is the valence sign of the ionic species. Concentrations are employed here, although it should be appreciated that intracellular ion activities (a_{ion}^i) may be required in certain experimental conditions when intracellular ionic activity

coefficients are considerably less than one. $L_{S,S}$ is the straight coefficient describing the linear coupling of the substrate's forces to J_S , and $L_{ion,ion}$ describes the linear coupling of the cation's forces to J_{ion} . The cross coefficient $L_{S,ion}$ relates how flux of S is coupled to the nonconjugate driving forces of the cation ($\Delta\bar{\mu}_{ion}$) and $L_{ion,S}$ is the cross coefficient which relates the flux of the ion coupled to driving forces of S ($\Delta\mu_S$).

For the condition of completely efficient energetic coupling, J_S represents only cation-dependent flux of S , whereas J_{ion} represents only the S -dependent flux of the ion. By the Onsager (1931) symmetry relationship:

$$L_{ion,S} = L_{S,ion} \quad (3)$$

and subsequently the 'coupling coefficient' (number of moles of transported ion per mole transported S) is given by:

$$L_{S,ion} = J_{ion}/J_S. \quad (4)$$

Experimental methods for measuring the coupling coefficient are described below. In cells or membrane vesicles which accumulate S as a result of the experimentally imposed condition of an out \rightarrow in downhill flux of the ion, then:

$$|\Delta\bar{\mu}_{ion}L_{S,ion}| > \Delta\mu_S L_{S,S}. \quad (5)$$

In a non-equilibrium system (e.g. dissipating gradients in an oocyte, proteoliposome or membrane vesicle), then:

$$\Delta\mu_S/\Delta\bar{\mu}_{ion} = |L_{S,ion}/L_{S,S}|, \text{ when } J_S = 0. \quad (6)$$

This 'static head' condition described by equation 6 is experimentally exploited in the measurement of the coupling coefficient, as explained below.

In a perfectly efficient symporting system, there is no uncoupling (called internal slippage) or external leakage (paracellular diffusion), as discussed below. When such a system is at equilibrium, the rate of Gibbs free energy dissipation ($-dG/dt$) equals the sum of the flux \times force products for both species, and is given by:

$$-dG/dt = J_S\Delta\mu_S + J_{ion}\Delta\bar{\mu}_{ion} \geq 0 \quad (7)$$

and therefore:

$$J_S\Delta\mu_S \leq J_{ion}\Delta\bar{\mu}_{ion}. \quad (8)$$

Finally, it follows that the accumulated gradient of organic solute which can be sustained by $\Delta\bar{\mu}_{ion}$ across a membrane at equilibrium is:

$$\ln([S]^i/[S]^o) \leq L_{S,ion} \{ \ln([ion]^o/[ion]^i) - zF\Delta\Psi/RT \} \quad (9)$$

or:

$$[S]^i/[S]^o \leq \{ ([ion]^o/[ion]^i) e^{(-zF\Delta\Psi/RT)} \}^{L_{S,ion}}. \quad (10)$$

The inequality signs are included to describe the case of inefficiently coupled systems with shunt and slip pathways. Theoretically perfect coupling is not attained in biological membranes owing to external shunt pathways across leaky epithelial sheets of cells and to internal slip within the transporter that prevents the efficient coupling between J_S and J_{ion} . In the case of slip, the carrier may undergo an out \rightarrow in transmembrane translocation without S or ion or it may allow significant efflux of S .

Universal laws

It is well established that Na^+ , K^+ , H^+ , Cl^- and even lanthanide-series trivalent cations (Stevens and Kneer, 1988) can drive symport or antiport of a variety of solutes in many cell types of different species. Accumulation can be enhanced by additional coupling to $\Delta\Psi$. Although the above example is given for the case of cation-coupled symport with an uncharged solute, similar arguments hold whether the membrane involves complex systems of symport plus antiport, symport only or antiport only. This includes virtually all known ion-coupled transport systems that can be classified into various families and superfamilies in prokaryotes and eukaryotes (Kilberg *et al.* 1993; Maillard *et al.* 1994; Stevens, 1992a,b; Marger and Saier, 1993).

Steep concentration gradients measured across real membranes

Equations 9 and 10 predict that the solute concentrating ability of a system can involve both the chemical and electrical components of $\Delta\bar{\mu}_{\text{ion}}$. Indeed, a computer-generated surface plot of equation 10 is shown in Fig. 2 to emphasize visually that the concentrating ability of a symport system is greatly enhanced when the coupling coefficient and $\Delta\bar{\mu}_{\text{ion}}$ are compounded. Fig. 2 was generated by varying Na^+ concentrations in equation 10,

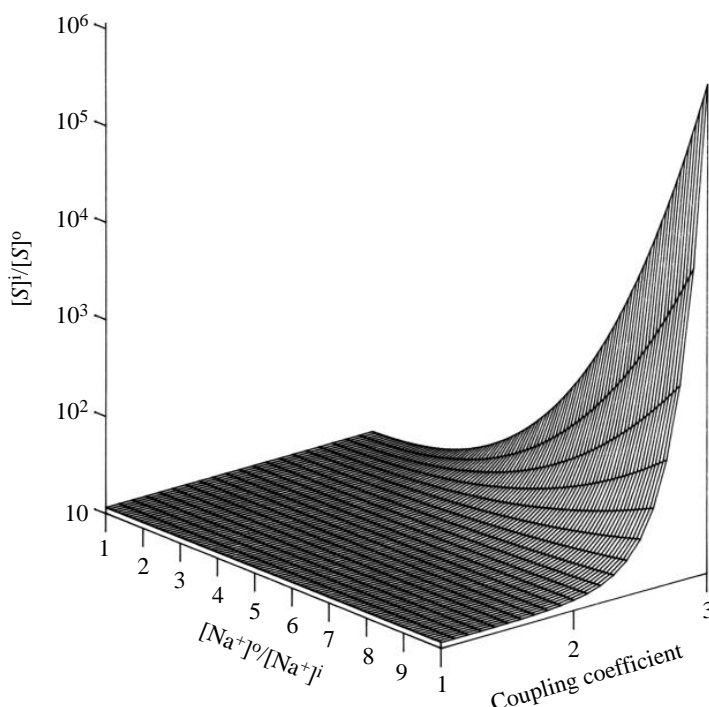


Fig. 2. Computer-generated surface plot of equation 10. The equation was generated with the condition that $\Delta\Psi$ remain fixed at -60 mV at 20°C . The resulting solute concentration gradients have been experimentally verified for neurotransmitters, amino acids and other solutes, as described in the text.

with the condition that $\Delta\Psi$ remains fixed at -60 mV at 20°C , and assuming that $\Delta\bar{\mu}_K$ contributes to $\Delta\Psi$. The generalization of Fig. 2 holds true for virtually any real $\Delta\Psi$. Note, for example, that the organic solute concentrating ability is about 100:1 for the condition of coupling coefficient $L_{S,\text{Na}}=1$ at $[\text{Na}^+]_{\text{ion}}^o/[\text{Na}^+]_{\text{ion}}^i=10$, and that by merely increasing the coupling coefficient $L_{S,\text{Na}}$ to 3, the system can sustain a solute gradient greater than 10^6 , as predicted by equation 10.

The model of Fig. 2 graphically demonstrates how many membrane systems – ranging from sugars in bacteria, to neurotransmitters in glia, neurons or synaptosomes, to amino acids in marine invertebrate epithelia – can support experimentally measured hundred-fold to million-fold steady-state concentration gradients of solutes (Clark and Amara, 1993; Preston and Stevens, 1982; Stephens, 1988; Stevens and Preston, 1980; Wright and Stephens, 1985; Ahearn and Behnke, 1991). Such membrane systems possess ion coupling coefficients of 2 or 3, with additional coupling to the electrical component (Manahan *et al.* 1983; Preston and Stevens, 1982; Schultz, 1980; Stephens, 1988; Wright *et al.* 1983; Wright and Stephens, 1985; Wright, 1987; Kaback *et al.* 1993; Clark and Amara, 1993). In the case of marine invertebrates, the measured high flux rates and free amino acid intracellular:extracellular steady-state concentration ratios of $10^6:1$ to $10^7:1$ arise from coupling uptake of 1 S to 3 Na^+ plus $\Delta\Psi$ (Preston and Stevens, 1982; Manahan *et al.* 1983). In the case of humans and other vertebrates, neurotransmitters such as glutamate, glycine and GABA are accumulated against steep gradients in neurons and glia coupled to Na^+ , K^+ and/or Cl^- chemical and electrical potentials (Hempling, 1993). Intracellular:extracellular measured concentration gradients of neurotransmitters in synaptosomes can exceed several thousand-fold in membrane systems known to couple neurotransmitter uptake to chemical and electrical gradients of multiple ion species (Hempling, 1993). In oocytes injected with GLAST-1 cRNA, glutamate transport is energized with a symport stoichiometry of 3Na^+ : 1 glutamate in exchange for 1K^+ antiport (Klockner *et al.* 1993). Several other high-affinity proteins associated with neurotransmitter uptake or re-uptake have been cloned (e.g. the GAT series, BGT-1, GLT-1, PROT-1, EAAC1), and some of these can be energized with multiple ion coupling stoichiometries of Na^+ , K^+ and/or Cl^- .

Measuring coupling

The stoichiometry of ion coupling can be experimentally measured by several techniques. The most straightforward techniques are based on equation 4, involving simultaneous measurement of S -dependent J_{ion} together with ion-dependent J_S using radiotracers.

Although directly measuring the coupling coefficient is theoretically straightforward (equation 4), in practice the absolute flux rates may be small, with low signal-to-noise ratios and large errors. This problem can be overcome if the flux rate for only one of the species is sufficiently high. For example, the rate of radiotracer S influx (J_S) at fixed $[S]^o$ can be measured as a function of $[\text{ion}]^o$, and the data can be fitted directly to the Hill equation (Segal, 1975):

$$J_S = J_{\text{max}} ([\text{ion}]^o)^n / \{ (K_{0.5})^n + ([\text{ion}]^o)^n \}. \quad (11)$$

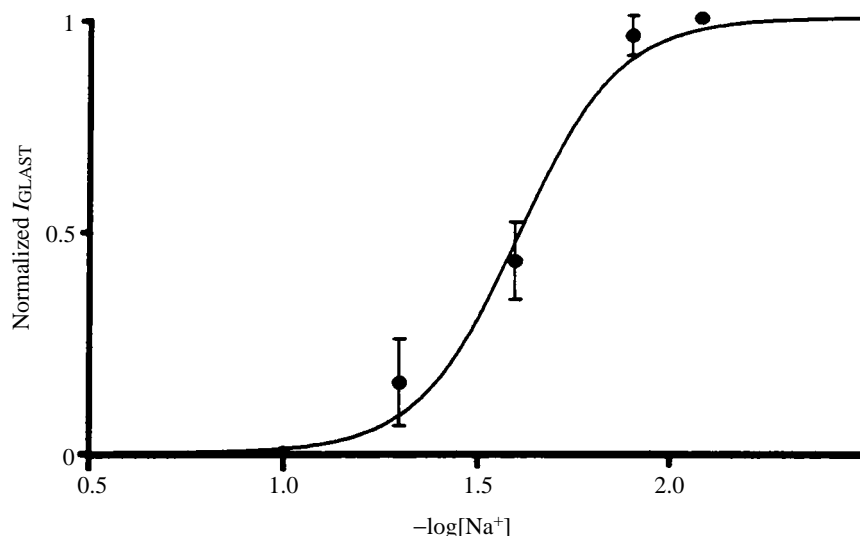


Fig. 3. Na^+ -activated inward currents in the presence of glutamate in oocytes injected with rat brain GLAST-1 cRNA. The amplitude of I_{GLAST} in the presence of constant 15 mol l^{-1} glutamate at increasing extracellular $[\text{Na}^+]$ gave the relationship of equation 11, with a Hill coefficient of 3.3. In similar experiments designed to measure I_{GLAST} as a function of $[\text{glutamate}]$ and $[\text{K}^+]$, the stoichiometry of the high-affinity sodium-dependent glutamate symport was $3\text{Na}^+ : 1$ glutamate in antiport exchange with 1K^+ (based on Klockner *et al.* 1993).

The value of the Hill coefficient, n , approximates the coupling coefficient in a cotransporting system that displays positive cooperativity, and $K_{0.5}$ represents the concentration of ion that gives half-maximal flux of solute. The value of n is best computed by non-linear regression of data fitted to equation 11. If the symport event is electrogenic, then inward currents attributable to the activator ion can be measured at fixed $[\text{S}]$. For example, the inward current induced by glutamate *via* GLAST-1 cRNA injected into oocytes (Klockner *et al.* 1993) gives a Hill number of 1 as a function of glutamate symport or K^+ antiport, but gives a Hill number of 3.3 as a function of $[\text{Na}^+]$ in the presence of constant $[\text{glutamate}]$. Therefore, the coupling stoichiometry is $3\text{Na}^+ : 1$ glutamate symport in exchange for 1K^+ (antiport) (Klockner *et al.* 1993). This example is shown in Fig. 3.

Measuring the ion activation of symport gives only the stoichiometry of activation and does not itself prove that the ion is cotransported with the other substrate. Furthermore, the Hill number may not be an exact integer, but may represent an estimate of the coupling coefficient, as is the case for $\text{Na}^+/\text{proline}$ symport, where the Hill number is 1.9 (Stevens and Wright, 1987), or $\text{Na}^+/\text{glucose}$ transport, where the Hill number is 1.6 (Wright, 1993). This disparity is due to theoretical limitations of the Hill equation which flaw the analysis (Segal, 1975) and to the fact that the actual coupling mechanism may not be energetically tight (i.e. there may be inefficiency or ‘slippage’ in the system, as discussed above).

Another way to estimate experimentally the coupling coefficient in a tightly coupled cotransporting system is the 'static head' application of equation 6. Using this technique, various net J_S values are measured in membrane vesicles or reconstituted proteoliposomes under solute-dissipating (non-equilibrium) conditions with variously imposed $\Delta\Psi$. In contrast to the activation method described above, the number of ion charges moved per mole of organic solute is measured under conditions of variously imposed $\Delta\bar{\mu}_{\text{ion}}$ and $\Delta\mu_S$, and the condition is sought whereby $J_S=0$. Turner (1985) has promoted static head experimental methods, whereby gradients are established by pre-loading membrane vesicles with sodium gluconate or SO_4^{2-} (final gradient $[\text{Na}^+]^o/[\text{Na}^+]^i=1$), radiolabeled S (at various gradients of $[S]^i/[S]^o$) and potassium gluconate or SO_4^{2-} {to clamp $\Delta\Psi$ in the presence of valinomycin according to the Nernst equation $\Delta\Psi=(RT/F)\ln([\text{K}^+]^i/[\text{K}^+]^o)$ }. The impermeant anions gluconate or SO_4^{2-} are used to reduce short-circuiting of $\Delta\Psi$. The J_S is subsequently measured by radiotracer efflux at various clamped $\Delta\Psi$. Under these conditions, the charge stoichiometry, q , approximately equals the coupling coefficient $L_{S,\text{Na}}$, and is thus computed directly from the condition $[S]^i/[S]^o=([\text{K}^+]^i/[\text{K}^+]^o)^q$. A control measurement made in the absence of Na^+ (substituting mannitol, choline or *N*-methyl-D-glucamine) measures the total Na^+ -independent J_S efflux. The actual static head condition occurs at the $\Delta\Psi$ that exactly counteracts the charges carried by Na^+ cotransported with the organic solute. That is, the imposed $[\text{K}^+]^i/[\text{K}^+]^o$ is sought which experimentally results in net $J_S=0$ (i.e. control). For example, in kidney brush-border membranes (Turner, 1985; Fukuhara and Turner, 1984), a 2:1 K^+ gradient is required to balance a 4:1 glucose gradient with a 1:1 Na^+ gradient, so that the coupling ratio is 2Na^+ :1 glucose.

Kinetic model of ion-coupled organic solute symport

Mechanistic models of symport/antiport are derived from both energetic and kinetic measurements. Fig. 4 describes a model of $\Delta\bar{\mu}_{\text{Na}}$ -activated solute binding and translocation in intestinal apical membranes. Considerable experimental evidence specifically supports the model for Na^+ /glucose symport, but it is recognized that a similar mechanism is likely to operate for other members of the SGLT-1 family of transporters (Stevens and Wright, 1985, 1987; Stevens, 1992*a,b*; Loo *et al.* 1993; Wright, 1993; Kimmich, 1990; Kessler and Semenza, 1983). The Cleland diagram of Na^+ /solute symport (Fig. 4) shows the dominant symport pathway and does not consider leak or slip paths for solute and Na^+ . This simplified model assumes net vectorial influx of one solute molecule activated with a 2Na^+ :1 solute coupling stoichiometry, assuming $\Delta\bar{\mu}_{\text{Na}}>0$ and $\Delta\Psi<0$. The unloaded carrier valence is -2 , and membrane voltage influences the binding of Na^+ to the carrier molecule as well as translocation rates of the loaded carrier. The binding of both sodium ions occurs before binding of S , and this is grouped as a single event in the simplified model. Binding sites for the membrane's extracellular side symporter C' combine with Na^+ and solute S to form the loaded complex $SC'\text{Na}_2$. This complex undergoes a conformational change that translocates S and Na^+ to the cytoplasmic side of the membrane $SC''\text{Na}_2$. The unloaded cytoplasmic conformation of the carrier site facing the cytoplasm C'' then reverts to the extracellular binding

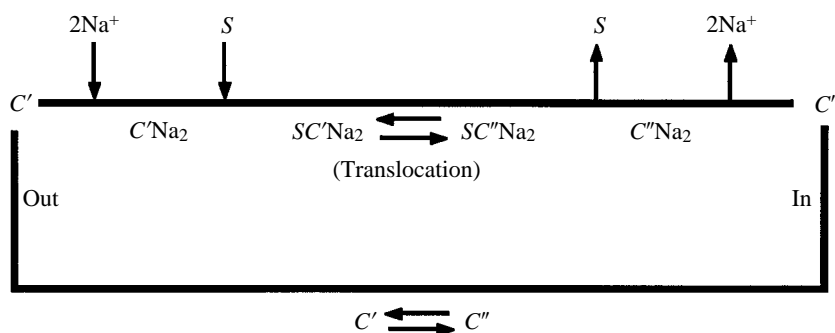


Fig. 4. Kinetic model of Na⁺/glucose symport or Na⁺/proline symport in epithelial membranes. This Cleland diagram describes an ordered kinetic model (Stevens and Wright, 1985, 1987; Stevens, 1992) based on steady-state radiotracer uptakes in apical membrane vesicles (Stevens and Wright, 1985, 1987; Kimmich, 1990; Kessler and Semenza, 1983). Wright's group (Wright, 1993; Loo *et al.* 1993) has confirmed the model specifically for Na⁺/glucose symport by measuring microscopic rate constants obtained by presteady-state current transients in oocytes injected with human SGLT-1. The inner leakage (slip) paths for Na⁺ alone or solute alone are considered to be insignificant at physiological concentrations, with $\Delta\bar{\mu}_{\text{Na}} > 0$. Net vectorial transport (out→in) of one solute molecule (S) is activated with a coupling stoichiometry of 2Na⁺:1 solute. Membrane voltage influences the binding of Na⁺ to carrier and translocation of carrier. The unloaded carrier valence is -2 . This simplified model shows binding of both sodium ions as a single event, with Na⁺ binding first to increase the carrier's affinity for solute (S). Sodium ions and S combine with the symporter's free binding sites at the lumen side (C') to form the loaded complex SC'Na₂. The loaded complex undergoes a conformational shift to SC''Na₂ that translocates Na⁺ and sugar to the cytoplasmic side of the membrane. Intracellular unloading events are poorly understood, although some experimental evidence suggests that S may unload before Na⁺ (Stevens and Wright, 1985, 1987). The unloaded carrier C'' subsequently isomerizes to a conformation that is ready to accept new substrates at the extracellular surface C'. Phlorizin binding to C'Na₂ prevents energetic coupling to $\Delta\bar{\mu}_{\text{Na}}$, thereby preventing secondary active transport. Wright's laboratory (Loo *et al.* 1993) has measured presteady-state forward and reverse rate constants for several of the steps.

conformation C', which can accept new substrates at the membrane's extracellular surface. Internal slippage and substrate leakage across the membrane (not shown in Fig. 4) would reduce the efficiency of coupling and could reduce the steady-state intracellular accumulation of solute. Additional details of this model are described in the legend of Fig. 4.

Functional unit arrangement of the symporter in the membrane

Some evidence suggests that polypeptides associated with transport may behave *in situ* in the membrane as a 'functional unit'. Polypeptide multimeric interactions may occur for intestinal or renal Na⁺/glucose symport, or for transport of substrates by the structurally homologous transport systems of the SGLT-1 family (systems serving nucleotides, myo-inositol or neutral amino acids in eukaryotes, and proline or pantothenic acid in bacteria).

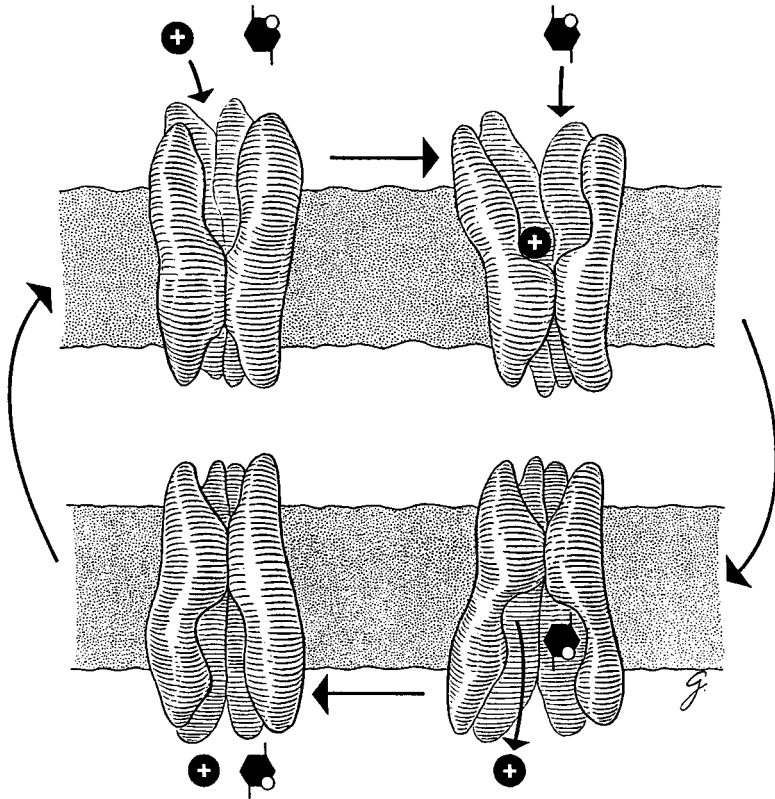


Fig. 5. Tentative physical model of the intestinal villus epithelial apical membrane-bound *in situ* functional Na⁺/glucose symporter. The size of the transporting functional unit is collectively 290kDa, consisting of intact, independent monomer subunits of about 70kDa each. These monomers may include SGLT-1 and RS1 arranged with unknown stoichiometry. For clarity, the circle with a net positive charge (collectively representing 2Na⁺ as in the case of the model of Fig. 4) plus 1 glucose molecule are shown interacting with the symporter functional unit. In this ordered binding model, kinetically described in Fig. 4, the extracellular sodium ions preferentially bind before organic solute, while the order of *trans* release of substrates is arbitrarily shown with Na⁺ being released first. In the final step, the symporter reverts to the conformation that optimally binds extracellular Na⁺ plus organic solute. The model is based on experiments employing electron radiation inactivation in conjunction with Western analysis using site-directed antibodies made against the cloned Na⁺/glucose SGLT-1 symporter, plus additional non-denaturing and denaturing Western analysis data (Veyhl *et al.* 1993) obtained using the RS1 cloned putative regulatory subunit and SGLT-1. Reproduced from Stevens *et al.* (1990) with permission.

Evidence for the functional multimer arrangement of the Na⁺/glucose symport system comes from several independent techniques. Keopsell's group (Veyhl *et al.* 1993) used antibodies raised against the cloned SGLT-1 protein (approximately 70kDa monomer) and against a cloned putative regulatory subunit of Na⁺/glucose symport (denoted RS1, approximately 70kDa monomer) to identify a 300kDa multimer by non-denaturing

Western analysis (Veyhl *et al.* 1993). Stevens *et al.* (1990) had previously shown, using Western analysis and transport activity in conjunction with radiation inactivation analysis, that the functional unit of the symporter *in situ* in the apical membrane is a composite of 70 kDa monomers giving a 290 kDa functional multimer. Stoichiometric co-injection of RS1 cRNA with SGLT-1 cRNA into an oocyte expression system indicated that both of these proteins were required for full expression of transport function that possessed physiological properties similar to those of the native intestinal membrane protein (Veyhl *et al.* 1993). Fig. 5 shows the *in situ* membrane-bound arrangement of the functional Na⁺/glucose symport system. The 290 kDa functional unit is a tetramer made up of four independent 70 kDa monomer subunits associated non-covalently. The stated evidence suggests that this is may be a heterotetramer, although alternative associations cannot be ruled out (e.g. dimer of RS1 and SGLT-1 homodimers). Koepsell's group showed that the maximal oocyte expression of glucose transport activity occurred when the cRNA molar ratio of RS1:SGLT-1 was 2; however, the stoichiometric distribution of these subunits within the 290 kDa transporting functional unit is unknown.

According to the kinetic model discussed in Fig. 4, two sodium ions bind and activate the transport functional unit shown in Fig. 5. After sodium and glucose or proline have bound, the functional unit undergoes a conformational shift that relocates the substrates to the cytoplasmic side. After Na⁺ and solute have been released, the symporter shifts back to a conformation that again favors binding of extracellular Na⁺ and solute. Ugolev and Metel'skii (1990) have suggested that, for Na⁺/glucose symport, the physical arrangement of the subunits may form individual conduits for Na⁺ and glucose.

Reversible work needed to maintain solute accumulation

In this section, we examine the individual roles of the chemical ($\Delta\mu_{\text{Na}} = RT \ln[\text{Na}^+]^o/[\text{Na}^+]^i$) and electrical ($zF\Delta\Psi$) components of $\Delta\bar{\mu}_{\text{Na}}$ in order to assess their energetic adequacy relative to the reversible work required to maintain neutral amino acids and sugars at cellular accumulation ratios greater than one. Sodium-activated solute transport in the foregut absorptive epithelial cells of *Aplysia californica* will serve as an example.

Although it is clear that the Na⁺ chemical gradient contributes significantly to the overall energy required for accumulative sugar and amino acid transport in *Aplysia* gut and other epithelia, the adequacy of $\Delta\mu_{\text{Na}}$ as the sole energy source for this purpose was questioned by Gerencser (1981a, 1983a, 1984). In the 1960s and 1970s, it had been demonstrated that, in the absence of mucosally applied organic solutes, small transepithelial potential differences (Ψ_{ms} , serosa positive) were normally observed across invertebrate gut wall (Gerencser, 1981a). The short-circuit current (I_{sc}) across animal gut preparations was accounted for either by a purely active absorptive Na⁺ current or by mixed active absorptive Na⁺ and Cl⁻ currents (Gerencser, 1981a). Subsequent addition of an accumulated sugar or amino acid to the mucosal aspect of animal gut preparations instantaneously enhance both Ψ_{ms} and I_{sc} (Schultz and Curran, 1970). In most cases, these observed electrical changes were accounted for by enhanced Na⁺ absorption (Gerencser, 1981b).

Table 1. Potential profile, intracellular K^+ and Na^+ activities and transmucosal K^+ and Na^+ electrochemical potential differences in *Aplysia californica* gut bathed in NaCl seawater medium

	Ψ_{ms} (mV)	Ψ_m (mV)	a_K^i (mmol l ⁻¹)	a_{Na}^i (mmol l ⁻¹)	$\Delta\bar{\mu}_K/F$ (mV)	$\Delta\bar{\mu}_{Na}/F$ (mV)
Mean	-1.3	-55.3	383	17.2	43	-129
±S.E.M.	±0.4	±2.2	±15	±2.5		
<i>N</i>		89	42	16		
<i>n</i>	11	11	7	4		

See text for abbreviations.

N, number of observations; *n*, number of animals.

Polarities of Ψ_{ms} and Ψ_m are relative to the mucosal solution. $\Delta\bar{\mu}_K/F$ and $\Delta\bar{\mu}_{Na}/F$ are calculated from equation 2 (Gerencsek, 1983a) using the mean Ψ_m , a_K^i and a_{Na}^i values.

Taken from Gerencsek (1983a), with permission.

Transmural events

Studies involving the effects of sugars (Gerencsek, 1978) or amino acids (Gerencsek, 1981b) on Na^+ absorption across the isolated gut of *Aplysia californica* revealed that mucosally applied organic solutes transported by secondary active transport (D-glucose, D-galactose, D-3-O-methylglucose, glycine, L-alanine and L-aminoisobutyric acid, AIB) instantaneously increased Ψ_{ms} and I_{sc} . These electrical effects were accounted for, in part, by means of an increase in the unidirectional mucosal-to-serosal (ms) flux of Na^+ (Gerencsek, 1978, 1981b). The addition of these same sugars or amino acids to the serosal aspect of the gut, at the same concentration, had virtually no effect on the transmural electrical characteristics, Ψ_{ms} and I_{sc} , nor on the unidirectional ms or sm fluxes of Na^+ (Gerencsek, 1978, 1981a,b). These results, coupled with the observation of the rapid nature of the organic solute-induced mucosal response (Gerencsek, 1978), suggest interaction of these solutes with specific components of the mucosal membrane. In addition, D-galactose (Table 3), glycine, AIB or L-alanine accumulation in the *Aplysia* gut tissue was shown to be absolutely dependent upon the presence of Na^+ in the seawater bathing medium, suggesting a reciprocal relationship between Na^+ and organic solute transport (Gerencsek, 1978, 1981a), as predicted by the Na^+ gradient hypothesis and observed in vertebrate gut (Schultz and Curran, 1970).

The net ms Na^+ transport by isolated *Aplysia* gut, in the absence of an electrochemical potential gradient, indicates that there is primary active transport of Na^+ in this preparation (Gerencsek, 1983a,b). This observation confirms a similar observation of net ms transfer of Na^+ across short-circuited *Aplysia* gut (Gerencsek, 1978). The observation that serosally applied ouabain inhibits the net absorptive flux of Na^+ , Ψ_{ms} and I_{sc} (Gerencsek, 1983a) strongly suggests that the endogenous electrical characteristics are dependent upon cellular ATP and its consequent hydrolysis by a ouabain-sensitive Na^+/K^+ -ATPase. These observations are consistent with the hypothesis that there is a Na^+/K^+ pump located within the basolateral membrane, which is responsible for uphill K^+ and Na^+ transport through this membrane and therefore for the maintenance of Ψ_{ms}

and I_{sc} . This hypothesis has been directly confirmed with the demonstration that Na^+/K^+ -ATPase activity is exclusively localized to the basolateral membrane in *Aplysia* foregut absorptive cells (Gerencser and Lee, 1985).

Intracellular events

Inasmuch as the Na^+ intracellular activity coefficient is considerably less than one in cells of *Aplysia* and other animals (Gerencser, 1983a,b, Walker and Brown, 1977), the energetic formalism presented above holds true, but the ion concentrations ($[\text{Na}^+]$) should be modified to a_{Na}^i and a_{Na}^o . To determine a_{Na}^i accurately by liquid ion-exchange microelectrode measurements, it is necessary to have a previous estimate of a_{K}^i . Therefore, K^+ -specific microelectrodes were advanced across the mucosal membrane of *Aplysia* foregut absorptive cells (Gerencser, 1983a,b). The calculated a_{K}^i obtained from these impalements averaged $383 \pm 15 \text{ mmol l}^{-1}$ (Table 1). Unlike the a_{K}^i measurements, Na^+ -specific microelectrodes advanced across the mucosal membrane of *Aplysia* foregut absorptive cells recorded negative potentials relative to the mucosal medium in every impalement; these changes in $\Delta\Psi$ are consistent with Na^+ existing below electrochemical equilibrium in the *Aplysia* cellular cytosol (Gerencser, 1983a,b). The calculated a_{Na}^i averaged $17.2 \pm 2.5 \text{ mmol l}^{-1}$ (Table 1). Also given in Table 1 are values for $\Delta\bar{\mu}_{\text{K}}$ and $\Delta\bar{\mu}_{\text{Na}}$, which clearly indicate that intracellular K^+ and Na^+ are far from electrochemical equilibrium across the *Aplysia* absorptive cell mucosal membrane. Thus, there is an electrochemical force of approximately 43 mV driving K^+ out of the cells and of 129 mV moving Na^+ into the cells, consistent with the operation of a basolaterally located Na^+/K^+ pump proposed in other epithelia (Schultz and Curran, 1970).

Intracellular concentrations of sodium ($[\text{Na}^+]^i$), and potassium ($[\text{K}^+]^i$), D-galactose, L-alanine, AIB and glycine, were obtained from the villous foregut absorptive cells of *Aplysia* gut (Gerencser, 1983a,b, 1984), as were the a_{Na}^i and a_{K}^i measurements. These measurements ensure reasonably valid activity coefficients $a_{\text{X}}^i/[\text{X}]^i$ for both Na^+ and K^+ when considering the structural and functional heterogeneity of the gut relative to villous, intervillous and crypt cell regions. As can be seen in Table 2, the experimental $a_{\text{Na}}^i/[\text{Na}^+]^i$ is much lower than that predicted for all cellular Na^+ being in free solution in the *Aplysia* absorptive cells. Approximately 30% of the intracellular Na^+ was bound or sequestered within the absorptive cells.

Table 2. Intracellular Na^+ and K^+ concentrations and activity coefficients

	$[\text{K}^+]^i$ (mequiv kg^{-1} cell water)	$a_{\text{K}}^i/[\text{K}^+]^i$	$[\text{Na}^+]^i$ (mequiv kg^{-1} cell water)	$a_{\text{Na}}^i/[\text{Na}^+]^i$	n
Mean	542	0.71	35.5	0.48	6
\pm S.E.	± 58		± 2.1		
N	12		12		

See text for abbreviations.

N , number of observations; n number of animals.

Taken from Gerencser (1983a), with permission.

Table 3. *Intracellular accumulation of electroneutral organic solutes across Aplysia californica gut*

	D-Galactose	L-Alanine	AIB	Glycine
[Cell]/[medium] (C/M)	6.3±0.4 (6)	6.1±0.5 (6)	6.6±0.4 (6)	19.7±2.7 (6)

Values are means ± S.E.M. Numbers in parentheses are numbers of observations.

All C/M concentrations ratios of the organic solutes have been corrected for extracellular water.

Taken from Gerencsek (1984), with permission.

AIB, aminoisobutyric acid.

Table 3 shows that there was a significant steady-state intracellular accumulation of all of the electroneutral organic solutes: D-galactose, L-alanine, AIB and glycine. Translating these data into transapical chemical potential differences for these organic solutes, $\Delta\mu_{\text{Gal}}$ (D-galactose), $\Delta\mu_{\text{Ala}}$ (L-alanine), $\Delta\mu_{\text{AIB}}$ (AIB) and $\Delta\mu_{\text{Gly}}$ (glycine), and transposing the previously derived $\Delta\mu_{\text{Na}}$ and $\Delta\bar{\mu}_{\text{Na}}$ into a composite table (Table 4), one can compare the reversible work, in J mol^{-1} , required to transfer one equivalent of Na^+ or organic solute across the mucosal membrane of an *Aplysia* villous absorptive cell. As can be seen in Table 4, $\Delta\mu_{\text{Na}}$ is energetically adequate to drive the intracellular accumulation of all the organic solutes except glycine. However, the energy implicit within $\Delta\bar{\mu}_{\text{Na}}$ is thermodynamically adequate for the steady-state accumulation of glycine and the other organic solutes into the *Aplysia* foregut absorptive cell. Therefore, the glycine case exemplifies and highlights the situation in which $\Delta\Psi$ can be (and sometimes has to be)

Table 4. *Comparison of the reversible work ($\Delta\mu_{\text{organic solute}}$) required to achieve a steady-state cell/medium organic solute concentration in epithelial cells of Aplysia californica gut with the maximum reversible work obtainable from the chemical ($\Delta\mu_{\text{Na}}$) and electrochemical ($\Delta\bar{\mu}_{\text{Na}}$) transapical Na^+ gradients and the corresponding K^+ electrochemical gradient ($\Delta\bar{\mu}_{\text{K}}$) under the same conditions*

Gradient		Work (J mol^{-1})
$\Delta\mu_{\text{Na}}$	$RT\ln a_{\text{Na}}^i/a_{\text{Na}}^o$	7100
$\Delta\bar{\mu}_{\text{Na}}$	$\Delta\mu_{\text{Na}} + \Psi_m F$	12400
$\Delta\bar{\mu}_{\text{K}}$	$RT\ln a_{\text{K}}^i/a_{\text{K}}^o - \Psi_m F$	4200
$\Delta\mu_{\text{Gal}}$	$RT\ln [X]^i/[X]^o$	3400
$\Delta\mu_{\text{Ala}}$	$RT\ln [X]^i/[X]^o$	3300
$\Delta\mu_{\text{AIB}}$	$RT\ln [X]^i/[X]^o$	3600
$\Delta\mu_{\text{Gly}}$	$RT\ln [X]^i/[X]^o$	10600

All values are in J mol^{-1} organic solute or J equiv^{-1} Na^+ or K^+ transported across the mucosal membrane.

Values for $\Delta\bar{\mu}_{\text{Na}}$ and $\Delta\bar{\mu}_{\text{K}}$ are based on an average $\Psi_m = 55 \text{ mV}$.

Taken from Gerencsek (1984), with permission.

AIB, aminoisobutyric acid.

utilized as an energy source, in addition to $\Delta\mu_{\text{Na}}$, for the accumulation of organic solute relative to this and other cellular membrane systems.

Relative to other studies (Armstrong *et al.* 1979) regarding energetic adequacy of active organic solute accumulation in epithelia, the *Aplysia* gut demonstrates that $\Delta\mu_{\text{Na}}$ is energetically sufficient to drive uphill movement of sugar and amino acid into absorptive cells (Table 4), whereas in bullfrog gut $\Delta\mu_{\text{Na}}$ alone is not energetically sufficient to drive sugar uphill into the enterocyte. This physiological difference derives from the fact that there is a large disparity in $\Delta\mu_{\text{Na}}$ of the respective species. a_{Na}^i for both bullfrog and *Aplysia* gut cells are approximately the same; however, a_{Na}^o for *Aplysia* gut (sea water) approximates 306 mmol l^{-1} , whereas a_{Na}^o for bullfrog gut extracellular fluid approximates 76 mmol l^{-1} . Hence, the huge difference in $\Delta\mu_{\text{Na}}$ across the mucosal membranes of the two species is reflected in their different energetic requirements for driving organic solute uphill. It is worth adding that $\Delta\bar{\mu}_{\text{Na}}$ across the mucosal membrane of gut cells in both species is sufficient for their respective organic solute accumulation.

As referred to above, one major difficulty residing in the conclusive evaluation of the Na^+ gradient hypothesis as a mechanism for Na^+ -dependent solute transport is the uncertainty about the activity of intracellular Na^+ and its distribution in the cytoplasm. Some studies (Schultz and Curran, 1970) have equated the Na^+ gradient across the mucosal membrane to the ratio between mucosal bathing solution Na^+ concentration and the intracellular Na^+ concentration. This approach contains the following uncertainties. (1) Chemical determinations of intracellular Na^+ concentrations in tissues bathed in media with high Na^+ concentrations are affected drastically by relatively small errors in extracellular space measurement. This problem is seen in the wide variance of values for intracellular Na^+ concentrations reported in the literature from the 1960s and 1970s. (2) The assumption that all cellular water can be utilized as solvent water is questionable in several cell types. (3) In several cell types it is reasonably well established that intracellular Na^+ concentration does not reflect the true a_{Na}^i (Armstrong and Lee, 1971; Gerencser, 1983*a,b*). Most of these difficulties can be circumvented by the use of ion-selective microelectrodes, which would directly determine a_{Na}^i , and therefore $\Delta\bar{\mu}_{\text{Na}}$, across the biomembrane, and this could then be applied to ascertain the true energetic adequacy to the active uptake of solutes as stated in the Na^+ gradient hypothesis.

References

- AHEARN, G. A. AND BEHNKE, R. D. (1991). L-Proline transport systems of starfish pyloric caeca *J. exp. Biol.* **158**, 477–493.
- ARMSTRONG, W. MCD. AND LEE, C. O. (1971). Sodium and potassium activities in normal and 'Sodium Rich' frog skeletal muscle. *Science* **171**, 413–415.
- ARMSTRONG, W. MCD., BIXENMAN, W. R., FREY, K. F., GARCIA-DIAZ, J. G., O'REGAN, M. G. AND OWENS, J. L. (1979). Energetics of coupled Na^+ and Cl^- entry into epithelial cells of bullfrog small intestine. *Biochim. biophys. Acta* **551**, 207–219.
- CHRISTENSEN, H. N. (1990). Role of amino acid transport and countertransport in nutrition and metabolism. *Physiol. Rev.* **70**, 43–77.
- CHRISTENSEN, H. N. AND RIGGS, T. R. (1952). Concentrative uptake of amino acids by the Ehrlich mouse ascites carcinoma cell. *J. biol. Chem.* **194**, 57–68.
- CLARK, J. A. AND AMARA, S. G. (1993). Amino acid neurotransmitter transporters: structure, function and molecular diversity. *BioEssays* **15**, 323–332.

- CRANE, R. K. (1977). The gradient hypothesis and other models of carrier-mediated active transport. *Rev. Physiol. Biochem. Pharmac.* **78**, 101–159.
- CRANE, R. K., MILLER, D. AND BIHLER, I. (1961). The restrictions on the possible mechanism of intestinal active transport of sugars. In *Membrane Transport and Metabolism* (ed. A. Kotyk), pp. 439–449. Prague: Czechoslovakian Academy of Sciences Press.
- FUKUHARA, Y. AND TURNER, R. J. (1984). The static head method for determining the charge stoichiometry of coupled transport systems. Applications to the sodium-coupled D-glucose transporters of the renal proximal tubule. *Biochim. biophys. Acta* **770**, 73–78.
- GERENCSEK, G. A. (1978). Enhancement of sodium and chloride transport by monosaccharides. In *Aplysia californica* intestine. *Comp. Biochem. Physiol.* **61A**, 203–208.
- GERENCSEK, G. A. (1981a). Review: Intestinal potentials. *Comp. Biochem. Physiol.* **69A**, 15–21.
- GERENCSEK, G. A. (1981b). Effects of amino acids on chloride transport in *Aplysia* intestine. *Am. J. Physiol.* **240**, R61–R69.
- GERENCSEK, G. A. (1983a). Na⁺ absorption in *Aplysia* intestine: Na⁺ fluxes and intracellular Na⁺ and K⁺ activities. *Am. J. Physiol.* **244**, R412–R417.
- GERENCSEK, G. A. (1983b). Electrophysiology of chloride transport in *Aplysia* intestine. *Am. J. Physiol.* **244**, R143–R149.
- GERENCSEK, G. A. (1984). Transapical Na⁺ electrochemical potential difference and solute accumulation in *Aplysia californica* enterocytes. *Comp. Biochem. Physiol.* **78A**, 137–140.
- GERENCSEK, G. A. AND LEE, S. H. (1985). Cl⁻-HCO₃⁻ stimulated ATPase in intestinal mucosa of *Aplysia*. *Am. J. Physiol.* **248**, R241–R248.
- HEINZ, E., GECK, P. AND WILBRANDT, W. (1972). Coupling in secondary active transport activation of transport by co-transport and or counter-transport with the fluxes of other solutes. *Biochim. biophys. Acta* **255**, 442–461.
- HEMPLING, H. G. (1993). Analyzing an electrogenic cotransporter. *J. Membr. Biol.* **134**, 225–230.
- KABACK, R. H., JUNG, K., JUNG, H., WU, J., PRIVE, G. G. AND ZEN, K. (1993). What's new with lactose permease. *J. Bioenerg. Biomembr.* **25**, 627–636.
- KATCHALSKY, A. (1960). Membrane permeability and the thermodynamics of irreversible processes. In *Membrane Transport and Metabolism* (ed. A. Kleinzeller and A. Kotyk), pp. 69–80. London: Academic Press.
- KEDEM, O. (1978). Classification of transport mechanisms by non-equilibrium thermodynamics. In *Transport by Proteins*, pp. 15–26, Berlin: Walter de Gruyter and Co.
- KESSLER, M. AND SEMENZA, G. (1983). The small-intestinal Na⁺, D-glucose cotransporter: an asymmetric gated channel (or pore) responsive to Dy. *J. Membr. Biol.* **76**, 27–56.
- KILBERG, M. S., STEVENS, B. R. AND NOVAK, D. A. (1993). Recent advances in mammalian amino acid transport. *A. Rev. Nutr.* **13**, 137–165.
- KIMMICH, G. A. (1990). Membrane potentials and the mechanism of intestinal Na⁺-dependent sugar transport. *J. Membr. Biol.* **114**, 1–27.
- KLOCKNER, U., THORSTEN, S., CONRADT, M. AND STOFFEL, W. (1993). Electrogenic L-glutamate uptake in *Xenopus laevis* oocytes expressing a cloned rat brain L-glutamate/L-aspartate transporter (Glast-1). *J. Biol. Chem.* **268**, 14594–14596.
- LOO, D. D., HAZAMA, A., SUPPLISSON, S., TURK, E. AND WRIGHT, E. M. (1993). Relaxation kinetics of the Na⁺/glucose cotransporter. *Proc. natn. Acad. Sci. U.S.A.* **90**, 5767–771.
- MAILLIARD, M., STEVENS, B. R. AND MANN, G. (1994). Amino acid transport in the pancreas, liver and small intestine. *Gastroenterology* (in press).
- MANAHAN, D. T., DAVIS, J. P. AND STEPHENS, G. C. (1983). Bacteria-free sea urchin larvae: selective uptake of neutral amino acids from seawater. *Science* **220**, 204–206.
- MARGER, M. D. AND SAIER, M. H. (1993). A major superfamily of transmembrane facilitators that catalyse uniport, symport and antiport. *Trends physiol. Sci.* **18**, 13–20.
- MITCHELL, P. (1961). Coupling of phosphorylation to electron hydrogen transfer by a chemiosmotic type mechanism. *Nature* **191**, 144–148.
- MITCHELL, P. (1991). Foundations of vectorial metabolism and osmochemistry. *Biosci. Rep.* **11**, 297–344.
- ONAGER, L. (1931). Reciprocal relations in irreversible processes. *Phys. Rev.* **38**, 2265–2279.
- PRESTON, R. L. AND STEVENS, B. R. (1982). Kinetic and thermodynamic aspects of sodium-coupled amino acid transport acid transport by marine invertebrates. *Am. Zool.* **22**, 709–721.

- RIGGS, T. R., WALTER, L. M. AND CHRISTENSEN, H. N. (1958). Potassium migration and amino acid transport. *J. biol. Chem.* **233**, 1479–1484.
- SCHULTZ, S. G. (1980). *Basic Principles of Membrane Transport*. Cambridge: Cambridge University Press. 144pp.
- SCHULTZ, S. G. AND CURRAN, P. F. (1970). Coupled transport of sodium and organic solutes. *Physiol. Rev.* **50**, 631–718.
- SEGAL, I. H. (1975). *Enzyme Kinetics*. New York: John Wiley and Sons, Inc., 957pp.
- STEIN, W. D. (1986). *Transport and Diffusion Across Cell Membranes*. Orlando: Academic Press. 685pp.
- STEPHENS, G. C. (1988). Epidermal amino acid transport in marine invertebrates. *Biochim. biophys. Acta* **947**, 113–138.
- STEVENS, B. R. (1992a). Vertebrate intestinal apical membrane mechanisms of organic nutrient transport. *Am. J. Physiol.* **263**, R458–R463.
- STEVENS, B. R. (1992b). Amino acid transport in intestine. In *Mammalian Amino Acid Transport: Mechanisms and Control* (ed. M. S. Kilberg and D. Haussinger), pp. 149–164. New York: Plenum Press.
- STEVENS, B. R., KAUNTIZ, J. D. AND WRIGHT, E. M. (1984). Intestinal transport of amino acids and sugars: advances using membrane vesicles. *A. Rev. Physiol.* **46**, 417–433.
- STEVENS, B. R. AND KNEER, C. K. (1988). Lanthanide stimulated glucose and proline transport across rabbit intestinal brush border membranes. *Biochim. biophys. Acta* **942**, 205–208.
- STEVENS, B. R. AND PRESTON, R. L. (1980a). Sodium-dependent steady-state L-alanine accumulation by the body wall of *Glycera dibranchiata*. *J. exp. Zool.* **212**, 139–146.
- STEVENS, B. R. AND PRESTON, R. L. (1980b). The effect of sodium on the kinetics of L-alanine influx by the integument of *Glycera dibranchiata*. *J. exp. Zool.* **212**, 129–138.
- STEVENS, B. R. AND WRIGHT, E. M. (1985). Kinetic model of the intestinal brush border sodium/proline (IMINO) cotransporter. *N.Y. Acad. Sci.* **456**, 115–117.
- STEVENS, B. R. AND WRIGHT, E. M. (1987). Kinetics of the intestinal brush border proline (Imino) carrier. *J. biol. Chem.* **262**, 6546–6551.
- STEVENS, B. R., FERNANDEZ, A., HIRAYAMA, B., WRIGHT, E. M. AND KEMPNER, E. S. (1990). Intestinal brush border membrane Na⁺/glucose cotransporter functions *in situ* as a homotetramer. *Proc. natn. Acad. Sci. U.S.A.* **87**, 1456–1460.
- TURNER, R. J. (1985). Stoichiometry of co-transport systems. *Ann. N.Y. Acad. Sci.* **456**, 10–25.
- UGOLEV, A. M. AND METEL'SKII, S. T. (1990). Two channel transporter versus a single-channel Na⁺-dependent transporter for glucose and amino acids in rat and turtle. *Biomed. Sci.* **1**, 578–584.
- VEYHL, M., SPANGENBERG, J., PUSCHEL, B., POPPE, R., DEKEL, C., FRITZSCH, G., HAASE, W. AND KOEPESELL, H. (1993). Cloning of a membrane-associated protein which modifies activity and properties of the Na⁺-D-glucose cotransporter. *J. biol. Chem.* **268**, 25041–25053.
- WALKER, J. L. AND BROWN, H. M. B. (1977). Intracellular ionic activity measurements in nerve and muscle. *Physiol. Rev.* **57**, 729–778.
- WRIGHT, E. M. (1993). The intestinal Na⁺/glucose cotransporter. *A. Rev. Physiol.* **55**, 575–589.
- WRIGHT, S. H. (1987). Alanine and taurine transport by the gill epithelium of a marine bivalve: effect of sodium on influx. *J. Membr. Biol.* **95**, 37–45.
- WRIGHT, S. H., HIRAYAMA, B., KAUNTIZ, J. D., KIPPEN, I. AND WRIGHT, E. M. (1983). Kinetics of sodium succinate cotransport across renal brush border membranes. *J. biol. Chem.* **258**, 5456–5462.
- WRIGHT, S. H. AND STEPHENS, G. C. (1985). In *Transport Processes, Iono- and Osmoregulation: Current Comparative Approaches* (ed. R. Gilles and M. Gilles-Baillien), pp. 292–302. Heidelberg: Springer-Verlag.